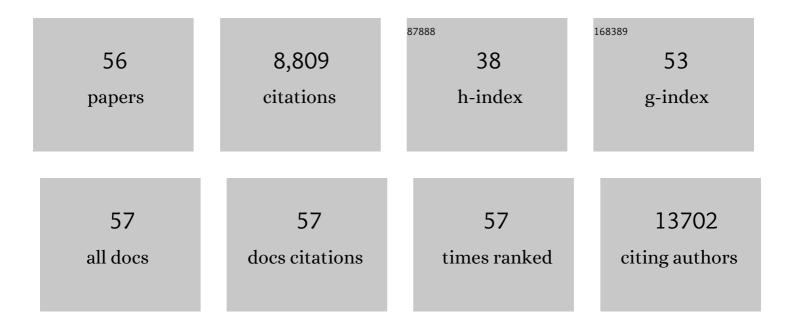
Hongtao Sun

List of Publications by Year in descending order

Source: https://exaly.com/author-pdf/8741120/publications.pdf Version: 2024-02-01



ΗΟΝΟΤΛΟ SUN

#	Article	IF	CITATIONS
1	Vacuumâ€Dried 3D Holey Graphene Frameworks Enabling High Mass Loading and Fast Charge Transfer for Advanced Batteries. Energy Technology, 2020, 8, 1901002.	3.8	8
2	Hierarchical Porous Carbon Derived from Covalent Triazine Frameworks for High Mass Loading Supercapacitors. , 2019, 1, 320-326.		29
3	Differential Surface Elemental Distribution Leads to Significantly Enhanced Stability of PtNi-Based ORR Catalysts. Matter, 2019, 1, 1567-1580.	10.0	82
4	Ultra-high Areal Capacity Realized in Three-Dimensional Holey Graphene/SnO2 Composite Anodes. IScience, 2019, 19, 728-736.	4.1	40
5	Single-atom tailoring of platinum nanocatalysts for high-performance multifunctional electrocatalysis. Nature Catalysis, 2019, 2, 495-503.	34.4	464
6	Facile and scalable preparation of 3D SnO ₂ /holey graphene composite frameworks for stable lithium storage at a high mass loading level. Inorganic Chemistry Frontiers, 2019, 6, 1367-1373.	6.0	19
7	Double-negative-index ceramic aerogels for thermal superinsulation. Science, 2019, 363, 723-727.	12.6	429
8	Hierarchical 3D electrodes for electrochemical energy storage. Nature Reviews Materials, 2019, 4, 45-60.	48.7	554
9	General synthesis and definitive structural identification of MN4C4 single-atom catalysts with tunable electrocatalytic activities. Nature Catalysis, 2018, 1, 63-72.	34.4	1,476
10	Three-dimensional holey-graphene/niobia composite architectures for ultrahigh-rate energy storage. Science, 2017, 356, 599-604.	12.6	1,229
11	Three-Dimensional Holey-Graphene/Niobia Composite Architectures for Ultrahigh-Rate Energy Storage. ECS Meeting Abstracts, 2017, , .	0.0	2
12	A hyperaccumulation pathway to three-dimensional hierarchical porous nanocomposites for highly robust high-power electrodes. Nature Communications, 2016, 7, 13432.	12.8	68
13	Stabilizing an amorphous V ₂ O ₅ /carbon nanotube paper electrode with conformal TiO ₂ coating by atomic layer deposition for lithium ion batteries. Journal of Materials Chemistry A, 2016, 4, 537-544.	10.3	57
14	Amorphous Ultrathin TiO ₂ Atomic Layer Deposition Films on Carbon Nanotubes as Anodes for Lithium Ion Batteries. Journal of the Electrochemical Society, 2015, 162, A974-A981.	2.9	53
15	Organic–Inorganic Heterointerfaces for Ultrasensitive Detection of Ultraviolet Light. Nano Letters, 2015, 15, 3787-3792.	9.1	117
16	Highly thermally conductive and mechanically strong graphene fibers. Science, 2015, 349, 1083-1087.	12.6	564
17	Graphene-Wrapped Mesoporous Cobalt Oxide Hollow Spheres Anode for High-Rate and Long-Life Lithium Ion Batteries. Journal of Physical Chemistry C, 2014, 118, 2263-2272.	3.1	119
18	Ultrathin gold island films for time-dependent temperature sensing. Journal of Nanoparticle Research, 2014, 16, 1.	1.9	4

Hongtao Sun

#	Article	IF	CITATIONS
19	Largeâ€Area Freestanding Graphene Paper for Superior Thermal Management. Advanced Materials, 2014, 26, 4521-4526.	21.0	386
20	Rapid synthesis of nitrogen-doped graphene for a lithium ion battery anode with excellent rate performance and super-long cyclic stability. Physical Chemistry Chemical Physics, 2014, 16, 1060-1066.	2.8	146
21	Amorphous vanadium oxide coating on graphene by atomic layer deposition for stable high energy lithium ion anodes. Chemical Communications, 2014, 50, 10703.	4.1	61
22	High-rate lithiation-induced reactivation of mesoporous hollow spheres for long-lived lithium-ion batteries. Nature Communications, 2014, 5, 4526.	12.8	586
23	Advanced Phase Change Composite by Thermally Annealed Defect-Free Graphene for Thermal Energy Storage. ACS Applied Materials & Interfaces, 2014, 6, 15262-15271.	8.0	113
24	Flexible, thorn-like ZnO-multiwalled carbon nanotube hybrid paper for efficient ultraviolet sensing and photocatalyst applications. Nanoscale, 2014, 6, 13630-13636.	5.6	44
25	Bulk Iodoapatite Ceramic Densified by Spark Plasma Sintering with Exceptional Thermal Stability. Journal of the American Ceramic Society, 2014, 97, 2409-2412.	3.8	43
26	Synthesis of ZnO quantum dot/graphene nanocomposites by atomic layer deposition with high lithium storage capacity. Journal of Materials Chemistry A, 2014, 2, 7319-7326.	10.3	117
27	High-Performance Ultraviolet Photodetector Based on Organic–Inorganic Hybrid Structure. ACS Applied Materials & Interfaces, 2014, 6, 14690-14694.	8.0	62
28	Silica–Gold Core–Shell Nanosphere for Ultrafast Dynamic Nanothermometer. Advanced Functional Materials, 2014, 24, 2389-2395.	14.9	21
29	High quality ZnO–TiO 2 core–shell nanowires for efficient ultraviolet sensing. Applied Surface Science, 2014, 314, 872-876.	6.1	63
30	Electrospray deposition of a Co ₃ O ₄ nanoparticles–graphene composite for a binder-free lithium ion battery electrode. RSC Advances, 2014, 4, 1521-1525.	3.6	29
31	Porous Fe2O3 nanorods anchored on nitrogen-doped graphenes and ultrathin Al2O3 coating by atomic layer deposition for long-lived lithium ion battery anode. Carbon, 2014, 76, 141-147.	10.3	46
32	ZnO/graphene nanocomposite fabricated by high energy ball milling with greatly enhanced lithium storage capability. Electrochemistry Communications, 2013, 34, 312-315.	4.7	76
33	Pseudocapacitance of Amorphous TiO ₂ Thin Films Anchored to Graphene and Carbon Nanotubes Using Atomic Layer Deposition. Journal of Physical Chemistry C, 2013, 117, 22497-22508.	3.1	102
34	ZnO quantum dots-graphene composite for efficient ultraviolet sensing. Materials Letters, 2013, 112, 165-168.	2.6	21
35	Flexible free-standing graphene–TiO2 hybrid paper for use as lithium ion battery anode materials. Carbon, 2013, 51, 322-326.	10.3	156
36	3D WO3 nanowires/graphene nanocomposite with improved reversible capacity and cyclic stability for lithium ion batteries. Materials Letters, 2013, 108, 29-32.	2.6	51

Hongtao Sun

#	Article	IF	CITATIONS
37	High responsivity, fast ultraviolet photodetector fabricated from ZnO nanoparticle–graphene core–shell structures. Nanoscale, 2013, 5, 3664.	5.6	154
38	Effective Temperature Sensing by Irreversible Morphology Evolution of Ultrathin Gold Island Films. Journal of Physical Chemistry C, 2013, 117, 3366-3373.	3.1	34
39	Morphology controlled high performance supercapacitor behaviour of the Ni–Co binary hydroxide system. Journal of Power Sources, 2013, 238, 150-156.	7.8	175
40	Atomic layer deposition of amorphous TiO ₂ on graphene as an anode for Li-ion batteries. Nanotechnology, 2013, 24, 424002.	2.6	76
41	GRAPHENE AND GRAPHENE-BASED NANOCOMPOSITES: SYNTHESIS AND SUPERCAPACITOR APPLICATIONS. , 2012, , .		0
42	Displacive radiation-induced structural contraction in nanocrystalline ZrN. Applied Physics Letters, 2012, 101, 041904.	3.3	18
43	Temperature-Dependent Morphology Evolution and Surface Plasmon Absorption of Ultrathin Gold Island Films. Journal of Physical Chemistry C, 2012, 116, 9000-9008.	3.1	82
44	Atomic Layer Deposition of TiO ₂ on Graphene for Supercapacitors. Journal of the Electrochemical Society, 2012, 159, A364-A369.	2.9	186
45	Enhanced Ultraviolet Emission from Poly(vinyl alcohol) ZnO Nanoparticles Using a SiO ₂ –Au Core/Shell Structure. Nano Letters, 2012, 12, 5840-5844.	9.1	55
46	Surface plasmon resonances of Ga nanoparticle arrays. Applied Physics Letters, 2012, 101, 081905.	3.3	17
47	Flexible Pillared Grapheneâ€Paper Electrodes for Highâ€Performance Electrochemical Supercapacitors. Small, 2012, 8, 452-459.	10.0	297
48	Transmission Electron Microscopy Study of Eu-Doped Y ₂ O ₃ Nanosheets and Nanotubes. Nanoscience and Nanotechnology Letters, 2011, 3, 314-318.	0.4	0
49	Microstructural Analysis of a Laser-Processed Zr-Based Bulk Metallic Glass. Metallurgical and Materials Transactions A: Physical Metallurgy and Materials Science, 2010, 41, 1752-1757.	2.2	60
50	Formation and coarsening of Ga droplets on focused-ion-beam irradiated GaAs surfaces. Applied Physics Letters, 2009, 95, .	3.3	20
51	Laser deposition of a Cu-based metallic glass powder on a Zr-based glass substrate. Journal of Materials Research, 2008, 23, 2692-2703.	2.6	52
52	Influence of Implanted Aluminum Ions on the Oxidation Behavior of M5 Alloy at 500°C. Oxidation of Metals, 2006, 65, 377-390.	2.1	1
53	A New Y3Al5O12 Phase Produced by Liquid-Feed Flame Spray Pyrolysis (LF-FSP). Advanced Materials, 2005, 17, 830-833.	21.0	72
54	Epitaxial Magnetic Perovskite Nanostructures. Advanced Materials, 2005, 17, 2869-2872.	21.0	33

			C .	
\cap	NG	ΓΑΟ	-51	IN
U			00	

#	Article	IF	CITATIONS
55	Observation of Strained PdO in an Aged Pd/Ceria-Zirconia Catalyst. Catalysis Letters, 2002, 79, 99-105.	2.6	26
56	Aging-Induced Metal Redistribution in Bimetallic Catalysts. Catalysis Letters, 2002, 81, 1-7.	2.6	14